

Scintillation of Partially Coherent Light in Time Varying Complex Media

Josselin Garnier* Knut Sølna†

January 19, 2022

Abstract

We present a theory for wave scintillation in the situation with a time-dependent partially coherent source and a time-dependent randomly heterogeneous medium. Our objective is to understand how the scintillation index of the measured intensity depends on the source and medium parameters. We deduce from an asymptotic analysis of the random wave equation a general form of the scintillation index and we evaluate this in various scaling regimes. The scintillation index is a fundamental quantity that is used to analyze and optimize imaging and communication schemes. Our results are useful to quantify the scintillation index under realistic propagation scenarios and to address such optimization challenges.

*Centre de Mathématiques Appliquées, Ecole Polytechnique, 91128 Palaiseau Cedex, France (josselin.garnier@polytechnique.edu)

†Department of Mathematics, University of California, Irvine CA 92697 (ksolna@math.uci.edu)

Contents

1	Introduction	2
2	Probing Time-Dependent Complex Media with Partially Coherent Sources	5
2.1	Source and Medium Modeling	5
2.2	The Itô-Schrödinger Equation	6
2.3	Measurements and the Challenge of Understanding Scintillation .	8
3	Fourth-order Field Moment and Scintillation	9
4	Scintillation in Canonical Scaling Regimes	10
4.1	Source with Large Correlation Radius	10
4.2	Source with Intermediate Correlation Radius	13
4.3	Source with Small Correlation Radius	14
5	Example with Experimental Data	16
6	Conclusions	18
A	Analysis of Fourth-order Moment Equations	19
B	Derivation of Scintillation Results	21
B.1	Scintillation Regime with a Large Correlation Radius of the Source	21
B.2	Scintillation Regime with an Intermediate Correlation Radius of the Source	23
B.3	Scintillation Regime with a Small Correlation Radius of the Source	24

1 Introduction

We consider the fundamental problem of characterizing the scintillation of optical measurements with a time-dependent partially coherent source and a time-dependent random medium. The scintillation index corresponds to a measure of the signal-to-noise ratio or relative strength of fluctuations in the intensity. If I is the measured intensity (irradiance) then we define the scintillation index by

$$\mathcal{S} = \frac{\mathbb{E}[I^2] - \mathbb{E}[I]^2}{\mathbb{E}[I]^2}, \quad (1)$$

where $\mathbb{E}[\cdot]$ stands for the statistical expectation obtained by averaging over repeated measurements under independent and identically distributed conditions. Modeling and analysis of laser speckle and scintillation is a classic challenge in optics [10, 32, 1]. A rigorous mathematical analysis and quantification of scintillation has been a long standing open question despite the long history and importance of this challenge. General insight about what governs the scintillation is important in the design of optical systems, for instance for imaging

and communication through the turbulent atmosphere [27] and through oceanic turbulence [36]. The challenge of choosing appropriate sources for scintillation control has received a lot of attention [26].

In [19, 20] we presented an analysis of the scintillation problem for deterministic coherent beams and plane wave sources and time-independent media. In this paper we consider the scintillation problem when the source is partially coherent in time and space and the medium has time and space random fluctuations. Partially coherent sources have indeed been promoted for reducing scintillation at a receiving end in the context of laser propagation [29, 2, 35, 26]. Most of these studies rely on physical experiments or numerics and Monte Carlo simulations to evaluate the scintillation index. From the theoretical point of view, analysis of wave propagation can be carried out in a perturbative regime using in particular Rytov theory with small fluctuations in the wave field to obtain insight about the scintillation [30, 3]. The fluctuations of intensity over different receiver response times have been studied in [12, 6, 7] in the limits of very slow or very fast detectors. The effect of temporal coherence on scintillation for weak turbulence was considered in [13]. An analysis of scintillation and how it depends on the smoothness of deterministic initial condition is presented in [5] with a focus on understanding self-averaging situations with a vanishing scintillation index. Issues related to aperture averaging is also considered in [31] in the context of deterministic sources by using a path integral approach for modeling the effect of turbulence.

Here we consider the high-frequency and far-field situation where the effect of the random medium can be captured by a white-noise term in the Itô-Schrödinger equation that governs the evolution of the wave field [8, 9]. This equation can address both weak intensity fluctuations and strong intensity fluctuations (the saturated regime). The response time of the photodetector, the coherence times of the source and the random medium can be arbitrary, provided that they are larger than the travel time of the field from the source to the detector through the medium. Under such circumstances, the effective reduced system (45) for the fourth-order moments of the wave field can be derived from the Itô-Schrödinger equation and used for numerical evaluation of the scintillation index in the general high-frequency and far-field situation. Based on this system we obtain explicit expressions of the scintillation index in three scaling regimes determined by the ratio of the correlation radius of the source over the correlation radius of the medium. We then explicitly characterize scintillation with partially coherent sources and time-dependent random media and quantify how the space-time statistical parameters of the source and medium affect the scintillation index. An important aspect of our analysis is that we allow the medium to be time-dependent, so that it changes on a time scale that is slow relative to the travel time of the optical field. This is the situation in the context of laser beam propagation in the atmosphere with turbulence creating slow temporal changes of the medium. The detector in our modeling has a finite response time which can be on the time scale of the changes in the medium. The averaging at the detector can have a strong impact on the scintillation index depending on the characteristic time scales involved.

The configuration that we consider is illustrated in Figure 1 with a partially coherent source field impinging from the left and propagating through a random medium and then the scintillating intensity pattern is recorded at the receiver end. Our objective is to characterize the scintillation index of the observed transmitted intensity pattern shown to the right in the figure.

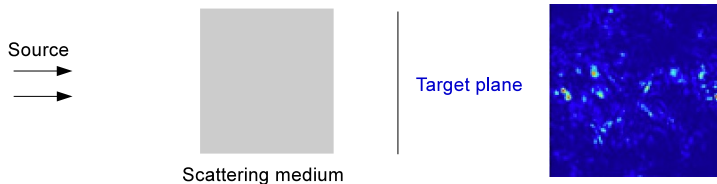


Figure 1: The figure shows the configuration that we consider. A partially coherent source fluctuating randomly in space and time is impinging on a complex medium. The complex medium is modeled as random and changes in time. The time changes in the medium happen on the recording time scale of the detector, but are slow relative to the travel time of the wave over the considered range. Due to time averaging the detector measures a smoothed version of the intensity and we seek to characterize the scintillation index of this measurement, which corresponds to a signal-to-noise ratio.

We comment on a special, but important, case corresponding to the wave field having a Gaussian distribution. Indeed it is a well-accepted conjecture that the statistics of the complex wave field becomes circularly symmetric complex Gaussian when the wave propagates through the turbulent atmosphere [33, 37] and the conjecture can be proved in certain situations [14, 4, 28]. In the Gaussian case the intensity is the sum of the squares of two independent Gaussian random variables, which up to a scaling has χ -square distribution with two degrees of freedom, that is, an exponential distribution. This situation gives a unit scintillation index. Based on an analysis of the fourth moment of the wave field we identify in this paper regimes that correspond to a unit value for the scintillation index and which are consistent with the Gaussian conjecture. The case with a Gaussian field distribution is the critical situation with the signal-to-noise ratio of the intensity being one. In general the scintillation index can be below one for small fluctuations in the intensity and can reach values beyond one when the intensity distribution has heavier tails than those corresponding to the exponential distribution. We encounter both situations in this paper and discuss what type of scaling regime may lead to such situations.

The outline of the paper is as follows. We formulate the problem in Section 2. This involves defining the statistical models for the source and the medium and deriving the stochastic partial differential equation, the Itô-Schrödinger equation, that characterizes the wave field. We then relate the solution of the stochastic partial differential equation to the measured scintillation index. The

main theoretical foundation for analyzing the scintillation is a framework for analyzing the fourth-order moment of the wave field and we discuss this in Section 3. In Section 4 we give the main results which characterize the scintillation index in various scaling regimes. In Section 5 we present an example involving data presented in [29]. Technical calculations associated with the fourth-order moment equations are presented in the appendices.

2 Probing Time-Dependent Complex Media with Partially Coherent Sources

In this section we outline the modeling and the problem that we will consider. In section 2.1 we describe the statistical modeling of the source and of the random medium. In section 2.2 we give the Itô-Schrödinger equation that describes the evolution of the wave field in the random medium. In section 2.3 we relate the random transmitted wave field to the quantity of interest which is the scintillation index of the measurements.

2.1 Source and Medium Modeling

The time-harmonic field $U(z, \mathbf{x}, t)$ satisfies the Helmholtz equation

$$\Delta U + k_o^2 n^2(z, \mathbf{x}, t)U = -\delta(z)f(\mathbf{x}, t), \quad (z, \mathbf{x}) \in \mathbb{R} \times \mathbb{R}^2, \quad (2)$$

where $k_o = 2\pi/\lambda_o$ is the central wavenumber (λ_o is the central wavelength). Here t is the slow time corresponding to the time at which the random medium and the source change. The coherence times of the medium and source are assumed to be much larger than the travel time from the source to the detector through the medium so that t is a frozen parameter in (2).

The source f in the plane $z = 0$ is partially coherent, statistically stationary in space and time. We model it as a complex Gaussian process with mean zero, variance one, and covariance

$$\mathbb{E}\left[f\left(\mathbf{x} + \frac{\mathbf{y}}{2}, t + \frac{\tau}{2}\right)\bar{f}\left(\mathbf{x} - \frac{\mathbf{y}}{2}, t - \frac{\tau}{2}\right)\right] = F\left(\frac{\tau}{\tau_s}\right)\exp\left(-\frac{|\mathbf{y}|^2}{4\ell_s^2}\right), \quad (3)$$

where ℓ_s , resp. τ_s , is the correlation radius, resp. the coherence time, of the source and the time covariance function F is normalized so that $F(0) = 1$ and $\int_0^\infty F(s)ds = 1$. Here the correlation radius of the source ℓ_s is assumed to be small relative to the range L and the coherence time τ_s is assumed to be much larger than the propagation time L/c_o , where c_o is the background speed of propagation and L is the distance from the source to the detector. For convenience we use here a Gaussian correlation function for the spatial source correlations, but we remark that we could have used a more general form. A more detailed model for the source, in particular a discussion of realization via Spatial Light Modulators (SLMs) can be found in [24, 2]. For other approaches to the generation of the partially coherent source we refer to [34] for instance.

The medium is random and we denote by ν the relative fluctuations in the square index of refraction: $n^2(z, \mathbf{x}, t) = 1 + \nu(z, \mathbf{x}, t)$. The stochastic process ν is stationary in space and time and zero-mean, and its covariance function is of the form

$$\mathbb{E}[\nu(z' + z, \mathbf{x}' + \mathbf{x}, t + \tau)\nu(z', \mathbf{x}', t)] = \sigma_m^2 G\left(\frac{\tau}{\tau_m}\right) \mathcal{C}_m\left(\frac{z}{\ell_m}, \frac{\mathbf{x}}{\ell_m}\right), \quad (4)$$

where ℓ_m , resp. τ_m , is the correlation radius, resp. the coherence time, of the random medium fluctuations, σ_m is the standard deviation of the fluctuations of the square index of refraction, and the functions G and \mathcal{C}_m are normalized so that $G(0) = 1$, $\int_0^\infty G(s)ds = 1$, $\mathcal{C}_m(0, \mathbf{0}) = 1$, $\int_{\mathbb{R}} \mathcal{C}_m(\zeta, \mathbf{0})d\zeta = 1$, and $\int_{\mathbb{R}^2} \mathcal{C}_m(0, \boldsymbol{\chi})d\boldsymbol{\chi} = 1$. The special case where the correlation function corresponds to Kolmogorov turbulence is discussed in [25]. Here the correlation radius of the random medium ℓ_m is assumed to be small relative to the range L and the coherence time of the medium τ_m is assumed to be much larger than the propagation time L/c_o . Thus, the ‘turnover time’ of the medium is long compared to the propagation time, however, we assume that it is on the scale of the coherence time of the source τ_s . Our interest is now in determining how the characteristics of these source and medium statistics determine the scintillation index of the transmitted wave field. We discuss next the equation that can be used to describe the evolution of the statistics of the wave field, that is, the equation that describes how the random scattering modifies the statistical distribution of the wave field from those of the source as the wave field propagates through the complex medium.

2.2 The Itô-Schrödinger Equation

The complex amplitude field u which modulates the carrier plane wave:

$$U(z, \mathbf{x}, t) = \frac{i}{2k_o} \exp(ik_o z)u(z, \mathbf{x}, t)$$

satisfies the Itô-Schrödinger equation [21]:

$$du(z, \mathbf{x}, t) = \frac{i}{2k_o} \Delta_{\mathbf{x}} u(z, \mathbf{x}, t) dz + \frac{ik_o}{2} u(z, \mathbf{x}, t) \circ dB(z, \mathbf{x}, t), \quad (5)$$

with the initial condition in the plane $z = 0$:

$$u(z = 0, \mathbf{x}, t) = f(\mathbf{x}, t).$$

Note that here $\Delta_{\mathbf{x}}$ is the transverse Laplacian and t is the slow time scale corresponding to the time at which the source and the random medium change and that it is a frozen parameter in (5). This is a consequence of our assumption that the coherence times of the source and of the medium are long relative to the travel time of the field over the range L . The derivation of Eq. (5) from Eq. (2) follows the lines of the proof presented in [21, 19] which deals with the case of a

time-independent medium. It is valid in the white-noise paraxial regime, when the wavelength is much smaller than the correlation radii of the source and of the medium, which are themselves much smaller than the propagation distance. Note that in (5) the symbol \circ stands for the Stratonovich stochastic integral, moreover, that $B(z, \mathbf{x}, t)$ is a real-valued Brownian field over $[0, \infty) \times \mathbb{R}^2 \times \mathbb{R}$ with a covariance that derives from the model for the medium fluctuations in (4)

$$\mathbb{E}[B(z, \mathbf{x}, t)B(z', \mathbf{x}', t')] = \sigma_m^2 \ell_m \min\{z, z'\} G\left(\frac{t-t'}{\tau_m}\right) C\left(\frac{\mathbf{x}-\mathbf{x}'}{\ell_m}\right), \quad (6)$$

where $C(\boldsymbol{\chi}) = \int_{\mathbb{R}} \mathcal{C}_m(\zeta, \boldsymbol{\chi}) d\zeta$, which is such that $C(\mathbf{0}) = 1$. The first- and second-order moments of the wave field solution of (5) has been studied in [21, 22]. The first-order moment of the wave field is zero. The second-order moment of the wave field (mutual coherence function) defined by

$$\mu_2(z, \mathbf{x}, \mathbf{y}; \tau) = \mathbb{E}\left[u\left(z, \mathbf{x} + \frac{\mathbf{y}}{2}, t + \tau\right) \overline{u\left(z, \mathbf{x} - \frac{\mathbf{y}}{2}, t\right)}\right] \quad (7)$$

satisfies [19]

$$\frac{\partial \mu_2}{\partial z} = \frac{i}{k_o} \nabla_{\mathbf{x}} \cdot \nabla_{\mathbf{y}} \mu_2 + \frac{k_o^2 \sigma_m^2 \ell_m}{4} U_2(\mathbf{x}, \mathbf{y}; \tau) \mu_2, \quad (8)$$

with the potential $U_2(\mathbf{x}, \mathbf{y}; \tau) = G(\tau/\tau_m) C(\mathbf{y}/\ell_m) - 1$ and the initial condition $\mu_2(z=0, \mathbf{x}, \mathbf{y}; \tau) = \mathbb{E}[f(\mathbf{x} + \mathbf{y}/2, t + \tau) f(\mathbf{x} - \mathbf{y}/2, t)]$ that are both independent on \mathbf{x} . The second-order moment is given by

$$\mu_2(z, \mathbf{x}, \mathbf{y}; \tau) = F\left(\frac{\tau}{\tau_s}\right) \exp\left[-\frac{|\mathbf{y}|^2}{4\ell_s^2} - \frac{\sigma_m^2 k_o^2 \ell_m z}{4} \left(1 - G\left(\frac{\tau}{\tau_m}\right) C\left(\frac{\mathbf{y}}{\ell_m}\right)\right)\right]. \quad (9)$$

By inspection of the behavior of the second-order moment when $\tau = 0$:

$$\mathbb{E}\left[u\left(z, \mathbf{x} + \frac{\mathbf{y}}{2}, t\right) \overline{u\left(z, \mathbf{x} - \frac{\mathbf{y}}{2}, t\right)}\right] = \exp\left[-\frac{|\mathbf{y}|^2}{4\ell_s^2} - \frac{\sigma_m^2 k_o^2 \ell_m z}{4} \left(1 - C\left(\frac{\mathbf{y}}{\ell_m}\right)\right)\right],$$

we find that the scattering mean free path ℓ_{mfp} (that is the typical propagation distance over which a coherent wave becomes incoherent) is

$$\ell_{\text{mfp}}^{-1} = \frac{\sigma_m^2 k_o^2 \ell_m}{8}. \quad (10)$$

Note that the scattering mean free path therefore is inversely proportional to the medium correlation length $\sigma_m^2 \ell_m$ characterizing the strength of the scattering. When C is smooth at zero: $C(\boldsymbol{\chi}) = 1 - c_2 |\boldsymbol{\chi}|^2 + o(|\boldsymbol{\chi}|^2)$, the correlation radius $\rho_c(z)$ of the wave field is

$$\rho_c^{-2}(z) = \ell_s^{-2} + \frac{c_2 \sigma_m^2 k_o^2 z}{\ell_m}. \quad (11)$$

By inspection of the behavior of the second-order moment when $\mathbf{y} = \mathbf{0}$:

$$\mathbb{E}\left[u(z, \mathbf{x}, t + \tau)\overline{u(z, \mathbf{x}, t)}\right] = F\left(\frac{\tau}{\tau_s}\right) \exp\left[-\frac{\sigma_m^2 k_o^2 \ell_m z}{4}\left(1 - G\left(\frac{\tau}{\tau_m}\right)\right)\right],$$

we can see that, when $F(s) = \exp(-s^2/4)$ and G is smooth at zero, $G(s) = 1 - g_2 s^2 + o(s^2)$, the coherence time $\tau_c(z)$ of the wave field is

$$\tau_c^{-2}(z) = \tau_s^{-2} + \frac{g_2 \sigma_m^2 k_o^2 \ell_m z}{\tau_m^2}. \quad (12)$$

Therefore, for deep probing both the correlation radius and coherence time of the wave field are proportional to the reciprocal of the square root of the propagation distance. We discuss next the measurements of intensity associated with the field u and the associated scintillation index.

2.3 Measurements and the Challenge of Understanding Scintillation

The intensity at lateral location \mathbf{x} in the plane $z = L$ of the photodetector is

$$I_T(\mathbf{x}) = \frac{1}{T} \int_0^T |u(L, \mathbf{x}, t)|^2 dt. \quad (13)$$

The intensity profile forms a smoothed speckle pattern. This smoothed speckle pattern depends in particular on the values of the integration time T , the coherence times of the source τ_s and of the medium τ_m and we aim to understand how.

The empirical scintillation index measured by the photodetector of total aperture A is

$$\mathcal{S} = \frac{\frac{1}{|A|} \int_A I_T(\mathbf{x})^2 d\mathbf{x} - \left(\frac{1}{|A|} \int_A I_T(\mathbf{x}) d\mathbf{x}\right)^2}{\left(\frac{1}{|A|} \int_A I_T(\mathbf{x}) d\mathbf{x}\right)^2}. \quad (14)$$

A more detailed model for the detector, in particular a discussion of the role of finite sized pixels of a (CCD) camera can be found in for instance [23, 29]. If the diameter of the photodetector aperture A is large (much larger than the speckle radius, i.e. the correlation radius), then

$$\mathcal{S} = \frac{\mathbb{E}[I_T(\mathbf{0})^2] - \mathbb{E}[I_T(\mathbf{0})]^2}{\mathbb{E}[I_T(\mathbf{0})]^2}, \quad (15)$$

which is equal to

$$\mathcal{S} = \frac{2}{T} \int_0^T \left(1 - \frac{\tau}{T}\right) \frac{\text{Cov}(|u(L, \mathbf{0}, 0)|^2, |u(L, \mathbf{0}, \tau)|^2)}{\mathbb{E}[|u(L, \mathbf{0}, 0)|^2]^2} d\tau, \quad (16)$$

which is our quantity of interest. Note that the expectation here and below refers to expectation with respect to both the randomness of the medium and of the source. Note also that it follows from [19] Section 5 that $\mathbb{E}[|u(L, \mathbf{0}, t)|^2] = 1$. Therefore, in order to analyze \mathcal{S} , it remains to compute the fourth-order moment $\mathbb{E}[|u(L, \mathbf{0}, 0)|^2 |u(L, \mathbf{0}, \tau)|^2]$. We discuss the task of computing this moment next.

3 Fourth-order Field Moment and Scintillation

It is convenient to introduce the notation

$$f_\tau = F\left(\frac{\tau}{\tau_s}\right), \quad g_\tau = G\left(\frac{\tau}{\tau_m}\right). \quad (17)$$

We also introduce a notation for the fourth moment

$$\mu_4(z, \mathbf{x}_1, \mathbf{x}_2, \mathbf{y}_1, \mathbf{y}_2; \tau) = \mathbb{E}\left[u(z, \mathbf{x}_1, t + \tau)\overline{u(z, \mathbf{y}_1, t + \tau)}\overline{u(z, \mathbf{x}_2, t)}\overline{u(z, \mathbf{y}_2, t)}\right]. \quad (18)$$

Here we focus on the fourth moment, while in [15] moments of all orders were considered under some simplifying assumptions of a different type. The fourth moment in (16) is a special case of the general fourth moment in (18) corresponding to evaluation at one spatial point only. The motivation for introducing the general fourth moment is that we can identify a partial differential equation satisfied by this general moment and we will subsequently discuss the simplification that follows from evaluating this at particular values for the arguments. The general fourth moment satisfies the equation

$$\frac{\partial \mu_4}{\partial z} = \frac{i}{2k_o} \left(\Delta_{\mathbf{x}_1} + \Delta_{\mathbf{x}_2} - \Delta_{\mathbf{y}_1} - \Delta_{\mathbf{y}_2} \right) \mu_4 + \frac{k_o^2 \sigma_m^2 \ell_m}{4} U_4(\mathbf{x}_1, \mathbf{x}_2, \mathbf{y}_1, \mathbf{y}_2; \tau) \mu_4, \quad (19)$$

with the generalized potential

$$\begin{aligned} U_4(\mathbf{x}_1, \mathbf{x}_2, \mathbf{y}_1, \mathbf{y}_2; \tau) &= C\left(\frac{\mathbf{x}_1 - \mathbf{y}_1}{\ell_m}\right) + C\left(\frac{\mathbf{x}_2 - \mathbf{y}_2}{\ell_m}\right) + g_\tau C\left(\frac{\mathbf{x}_1 - \mathbf{y}_2}{\ell_m}\right) \\ &+ g_\tau C\left(\frac{\mathbf{x}_2 - \mathbf{y}_1}{\ell_m}\right) - g_\tau C\left(\frac{\mathbf{x}_1 - \mathbf{x}_2}{\ell_m}\right) - g_\tau C\left(\frac{\mathbf{y}_1 - \mathbf{y}_2}{\ell_m}\right) - 2, \end{aligned} \quad (20)$$

and the initial condition:

$$\mu_4(z = 0, \mathbf{x}_1, \mathbf{x}_2, \mathbf{y}_1, \mathbf{y}_2; \tau) = \mathbb{E}\left[f(\mathbf{x}_1, t + \tau)\overline{f(\mathbf{y}_1, t + \tau)}\overline{f(\mathbf{x}_2, t)}\overline{f(\mathbf{y}_2, t)}\right].$$

This follows from (5) using Itô calculus for Hilbert space valued processes [20, 11]. Using the Gaussian property of the source and Isserlis formula, the initial condition for the fourth-order moment is:

$$\begin{aligned} \mu_4(z = 0, \mathbf{x}_1, \mathbf{x}_2, \mathbf{y}_1, \mathbf{y}_2; \tau) &= \exp\left(-\frac{|\mathbf{x}_1 - \mathbf{y}_1|^2}{4\ell_s^2} - \frac{|\mathbf{x}_2 - \mathbf{y}_2|^2}{4\ell_s^2}\right) \\ &+ f_\tau^2 \exp\left(-\frac{|\mathbf{x}_1 - \mathbf{y}_2|^2}{4\ell_s^2} - \frac{|\mathbf{x}_2 - \mathbf{y}_1|^2}{4\ell_s^2}\right). \end{aligned} \quad (21)$$

We can now express the quantity of interest, the scintillation index (16), in terms of the general fourth moment

$$\mathcal{S} = \frac{2}{T} \int_0^T \left(1 - \frac{\tau}{T}\right) \frac{\mu_4(L, \mathbf{0}, \mathbf{0}, \mathbf{0}, \mathbf{0}; \tau) - \mu_2(L, \mathbf{0}, \mathbf{0}; 0)^2}{\mu_2(L, \mathbf{0}, \mathbf{0}; 0)^2} d\tau, \quad (22)$$

where $\mu_2(L, \mathbf{0}, \mathbf{0}; 0) = \mathbb{E}[|u(L, \mathbf{0}, t)|^2] = 1$. Thus, it is the special fourth moment $\mu_4(L, \mathbf{0}, \mathbf{0}, \mathbf{0}; \tau)$ that is needed to analyze the scintillation index. The explicit solution of the problem (19) is not known. In some scaling regimes we can, however, identify asymptotic solutions using the framework introduced in [20]. In Appendix A we discuss a fundamental transformation of the fourth moment equation in (19) to a simplified problem from which the special fourth moment $\mu_4(L, \mathbf{0}, \mathbf{0}, \mathbf{0}; \tau)$ derives.

4 Scintillation in Canonical Scaling Regimes

We discuss here the three scaling regimes for the scintillation. In these regimes we can solve for the fourth moment in (19) explicitly. This allows us to get quantitative insight about the behavior of the scintillation and how it depends on the characteristic parameters in the problem and we comment on this in detail. The first two regimes are particular cases of the far-field (or Fraunhofer) regime $\frac{\lambda_o L}{\min(\ell_s, \ell_m)^2} \gg 1$, when scattering is moderate or strong $L \gtrsim \ell_{\text{mfp}}$. The third regime is a special Fresnel regime $\frac{\lambda_o L}{\min(\ell_s, \ell_m)^2} \sim 1$ when scattering is strong $L \gg \ell_{\text{mfp}}$. The parameter determining the different regimes of scintillation is the ratio of the correlation radius ℓ_s of the source over the correlation radius ℓ_m of the medium fluctuations.

4.1 Source with Large Correlation Radius

We consider first the regime in which the correlation radius ℓ_s of the source is larger than the correlation radius of the medium ℓ_m so that $\frac{\lambda_o L}{\ell_m^2} \gg 1$ but $\frac{\lambda_o L}{\ell_m \ell_s} \lesssim 1$. We carry out the analysis of this regime in Appendix B.1 where we derive the following expression for the scintillation index (22):

$$\mathcal{S} = \frac{2}{T} \int_0^T \left(1 - \frac{\tau}{T}\right) \left[f_\tau^2 \exp\left(-\frac{(1-g_\tau)\sigma_m^2 k_o^2 \ell_m L}{2}\right) + \mathcal{Q}_{g_\tau}(L) + f_\tau^2 \mathcal{Q}_1(L) \right] d\tau, \quad (23)$$

where the effective scattering kernel is given by

$$\begin{aligned} \mathcal{Q}_g(L) = & \exp\left(-\frac{\sigma_m^2 k_o^2 \ell_m L}{2}\right) \frac{1}{2\pi} \int_{\mathbb{R}^2} \exp\left(-\frac{|s|^2}{2}\right) \\ & \times \left[\exp\left(\frac{\sigma_m^2 k_o^2 \ell_m L g}{2} \int_0^1 C\left(\frac{L s s'}{k_o \ell_m \ell_s}\right) ds'\right) - 1 \right] ds. \end{aligned} \quad (24)$$

When $\frac{\lambda_o L}{\ell_m \ell_s} \ll 1$ the expression is simpler:

$$\mathcal{Q}_g(L) = \exp\left(-\frac{\sigma_m^2 k_o^2 \ell_m L}{2}(1-g)\right) - \exp\left(-\frac{\sigma_m^2 k_o^2 \ell_m L}{2}\right).$$

The kernel (24) depends on the two-point statistics of the random medium fluctuations and reflects cumulative scattering effects over the propagation distance L . Note that $g = 0$ corresponds to the situation with intensities of wave

fields having propagated through uncorrelated random media and that indeed $\mathcal{Q}_0(L) = 0$.

The first term in the square brackets in (23) corresponds to the scintillation contribution from the fluctuations of the source and this contribution is damped by temporal decorrelation of the medium fluctuations as well as temporal averaging at the detector. The second term in the square brackets is the scintillation contribution produced by the random medium fluctuations and is again damped by temporal decorrelation of the random medium fluctuations. The last term in the square brackets is a cross term reflecting the scintillation contribution from the combined effect of medium and source fluctuations.

We next discuss the behavior of the scintillation index in various special cases.

- Note first that a rapid decay of f_τ (short coherence time) corresponds to rapid decorrelation of the source. Such a rapid decorrelation serves to reduce the scintillation index due to averaging by the photodetector. Similarly rapid decay of g_τ corresponds to rapid decorrelation in the medium fluctuations and reduced scintillation due to averaging over incoherent scattering contributions. We find from (23) that when T becomes much larger than the coherence times of the source and of the medium, and assuming that $\tau \mapsto f_\tau \in L^2$ (i.e., is square-integrable) and that g_τ goes to zero at infinity fast enough so that $\tau \mapsto Q_{g_\tau}(L) \in L^1$ (i.e., is integrable), then we have

$$\mathcal{S} \xrightarrow{T \rightarrow +\infty} 0$$

for any propagation distance.

- An interesting situation corresponds to $g_\tau \equiv 1$, which means that the medium is frozen. We have

$$\frac{\mu_4(L, \mathbf{0}, \mathbf{0}, \mathbf{0}; \tau) - \mu_2(L, \mathbf{0}, \mathbf{0})^2}{\mu_2(L, \mathbf{0}, \mathbf{0})^2} = f_\tau^2 + (1 + f_\tau^2) \mathcal{Q}_1(L).$$

This means that, even if τ is so large that the initial fields are independent ($f_\tau = 0$) the intensities of the transmitted fields at the photodetector at different times are correlated, in fact the covariation degree is zero at $L = 0$, is not zero for positive L and goes to zero as $L \rightarrow +\infty$. The scintillation index is given by

$$\mathcal{S} = \frac{2}{T} \int_0^T \left(1 - \frac{\tau}{T}\right) \left[f_\tau^2 + (1 + f_\tau^2) \mathcal{Q}_1(L) \right] d\tau, \quad (25)$$

so that, when T becomes much larger than the coherence time of the source, and assuming that $f_\tau \in L^2$, then we have

$$\mathcal{S} \xrightarrow{T \rightarrow +\infty} \mathcal{Q}_1(L).$$

This shows that the scintillation index corresponding to averaging of the initial incoherent intensity is zero, while the one corresponding to the transmitted field is not.

- For τ smaller than both the coherence times of the source and the medium, we have $f_\tau = g_\tau = 1$ and then for T similarly small

$$\mathcal{S} = \frac{\mu_4(L, \mathbf{0}, \mathbf{0}, \mathbf{0}, \mathbf{0}; \tau) - \mu_2(L, \mathbf{0}, \mathbf{0}; 0)^2}{\mu_2(L, \mathbf{0}, \mathbf{0}; 0)^2} = 1 + 2\mathcal{Q}_1(L). \quad (26)$$

Thus, initially the scintillation index is one (because the source has Gaussian distribution), then it reaches beyond one in a mixing region and returns to one for large propagation distances. Indeed, the fluctuations of the initial field happen on a spatial scale that is large relative to the scale of the field variations that are imposed by the random medium fluctuations resulting in a non-Gaussian mixture situation with scintillation index beyond one.

- Consider the strongly scattering regime so that

$$\alpha_L := \frac{\sigma_m^2 k_o^2 \ell_m L}{2} \gg 1. \quad (27)$$

Note that then the propagation distance is larger than the scattering mean free path since $\alpha_L = 4L/\ell_{\text{mfp}}$, so that in the case of coherent sources most of the wave energy has been transferred to incoherent wave energy due to scattering. We will in the context of the strongly scattering regime (27) assume that C is smooth and isotropic so that we have (remember $C(\mathbf{0}) = 1$):

$$C(\boldsymbol{\chi}) = 1 - c_2 |\boldsymbol{\chi}|^2 + o(|\boldsymbol{\chi}|^2). \quad (28)$$

Then we we can compute a simplified expression for $\mathcal{Q}_1(L)$ and find

$$\mathcal{Q}_1(L) \stackrel{\alpha_L \gg 1}{\simeq} \frac{1}{1 + \frac{c_2 \sigma_m^2 L^3}{3 \ell_m \ell_s^2}},$$

so that $\mathcal{Q}_1(L)$ goes to zero when the propagation distance L becomes large.

In Figure 2 we illustrate the behavior of the scintillation in the regime $\ell_s \gg \ell_m$. The figure shows how the scintillation index in (26) depends on the propagation distance. We introduce the length parameter

$$\ell = \frac{\ell_m \ell_s}{\lambda_0}.$$

Then we show the scintillation index as function of L/ℓ for three different values of the medium fluctuation strength parameter

$$\alpha_\ell = \frac{\sigma_m^2 k_o^2 \ell_m \ell}{2},$$

when $C(\boldsymbol{\chi}) = \exp(-|\boldsymbol{\chi}|^2/2)$. Note that with stronger medium fluctuations the maximum value for the scintillation index is larger and happens for shorter propagation distances.

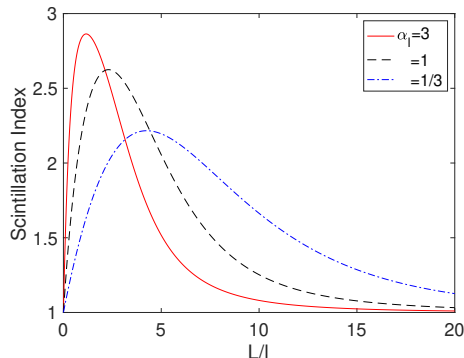


Figure 2: Scintillation index as a function of the relative propagation distance L/ℓ for three values of the medium fluctuation strength parameter α_ℓ . The figure corresponds to the regime $\ell_s \gg \ell_m$ for small averaging times at the detector so that the scintillation index is given by (26).

4.2 Source with Intermediate Correlation Radius

We consider next the case when the correlation radius of the source is of the same order as the correlation radius of the medium so that $\frac{\lambda_o L}{\ell_m^2} \gg 1$ and $\frac{\lambda_o L}{\ell_m \ell_s} \gg 1$. We carry out the analysis in Appendix B.2 where we derive the following expression for the scintillation index (22):

$$\mathcal{S} = \frac{2}{T} \int_0^T \left(1 - \frac{\tau}{T}\right) \left[f_\tau^2 \exp\left(-\frac{(1-g_\tau)\sigma_m^2 k_o^2 \ell_m L}{2}\right) \right] d\tau. \quad (29)$$

As above the term in the square brackets corresponds to scintillation contribution from the fluctuations in the source and this contribution is damped by fast temporal decorrelation of the medium fluctuations (small g_τ), moreover, by smoothing at the detector. Note that this term corresponds to the first term in the square brackets in (23). Indeed, the last two terms in the square brackets in (23) becomes small when ℓ_s is reduced so that $\frac{\lambda_o L}{\ell_m \ell_s} \gg 1$. The situation with $\ell_s \sim \ell_m$ is the regime considered here. If we further reduce ℓ_s so that $\ell_s \ll \ell_m$ then we may transition towards the regime considered in the next section. In the regime $\ell_s \sim \ell_m$ we can observe the following behaviors.

- In the case when T becomes much larger than the coherence time of the source, and assuming that $f_\tau \in L^2$, we have

$$\mathcal{S} \xrightarrow{T \rightarrow +\infty} 0$$

for any propagation distance due to averaging at the photodetector.

- For τ smaller than the coherence times of both the source and the medium, we have $f_\tau = g_\tau = 1$ and then with T similarly small

$$\mathcal{S} = 1.$$

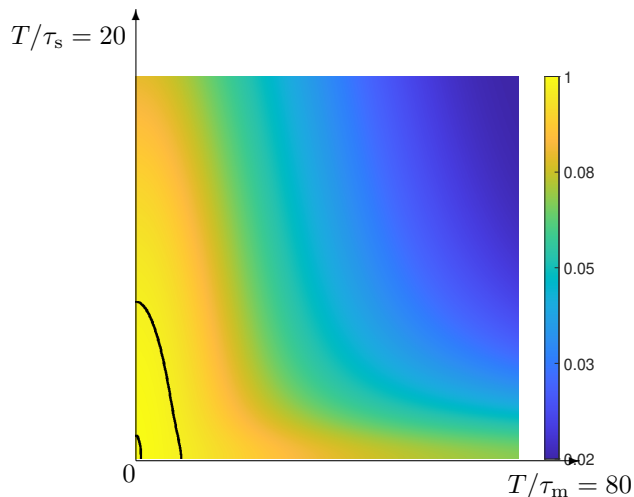


Figure 3: Scintillation index \mathcal{S} as a function of the coherence times of the source and of the random medium, respectively τ_s and τ_m , relative to T , the averaging time at the detector, in the regime $\ell_s \sim \ell_m$. The effective strength parameter for the magnitude of the medium fluctuations is $\alpha_L = \sigma_m^2 k_o^2 \ell_m L / 2 = 3$. The two solid black lines correspond to the contour levels $\mathcal{S} = .8$ and $.2$ respectively. Note that here and below we adapt the color scale to the particular distribution of scintillation index values.

Here the field behaves as a complex Gaussian field, because the fluctuations in the source and in the medium happen at the same scale.

In Figures 3 and 4 we illustrate the behavior of the scintillation index in the regime $\ell_s \sim \ell_m$. The figures show how the scintillation index depends on the magnitudes of the coherence times of the source and of the medium relative to the integration time at the detector. The two figures correspond to two different values for the strength of the medium fluctuations parameter α_L . The time coherence functions f_τ and g_τ are chosen to be Gaussian

$$f_\tau = \exp\left(-\frac{\tau^2}{2\tau_s^2}\right), \quad g_\tau = \exp\left(-\frac{\tau^2}{2\tau_m^2}\right). \quad (30)$$

Note how strong medium fluctuations serve to reduce the scintillation index in the case with a time-dependent random medium and temporal averaging at the detector, moreover, how also long duration detector temporal averaging serves to reduce the scintillation index.

4.3 Source with Small Correlation Radius

We finally consider the regime in which the correlation radius of the source is smaller than the correlation radius of the medium and we have $\frac{\lambda_o L}{\ell_s^2} \lesssim 1$. A

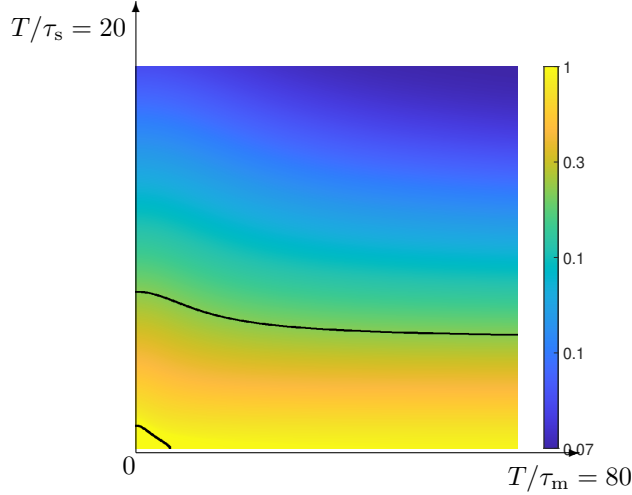


Figure 4: As in Figure 3, however with the medium fluctuation strength parameter $\alpha_L = \sigma_m^2 k_o^2 \ell_m L/2 = 1/3$.

similar regime (called spot-dancing regime) has already been considered in the literature to study coherent and narrow beam propagation: the beam propagates with the same transverse profile as in a homogeneous medium but its center randomly wanders, more exactly, its center is a random process whose standard deviation increases with propagation distance [19, 16]. Here, we also assume that C is smooth and isotropic with an expansion as in (28). We carry out the analysis in Appendix B.3 where we derive the following expression for the scintillation index (22):

$$\mathcal{S} = \frac{2}{T} \int_0^T \left(1 - \frac{\tau}{T}\right) \left[\frac{f_\tau^2}{1 + \frac{(1-g_\tau)c_2\sigma_m^2 L^3}{3\ell_m \ell_s^2}} \right] d\tau. \quad (31)$$

The numerator within the square brackets corresponds to the scintillation contribution of the Gaussian source, while the denominator corresponds to damping of the scintillation index due to temporal decorrelation in the random medium. We can moreover make the following observations.

- When T becomes much larger than the coherence time of the source, and assuming that $f_\tau \in L^2$, then we have

$$\mathcal{S} \xrightarrow{T \rightarrow +\infty} 0$$

for any propagation distance. Note that the scintillation index is small even if the medium is frozen since the medium fluctuations do not strongly contribute to the intensity correlations with the very small source correlation radius.

- For τ smaller than the coherence times of the source and of the medium, we have $f_\tau = g_\tau = 1$ and it follows that with T similarly small

$$\mathcal{S} = 1.$$

This corresponds to a Gaussian situation since the random medium fluctuations again does not strongly affect the correlations in this case with a source with rapid stationary spatial fluctuations. This is in contrast to the situation with a deterministic beam source when the spot dancing property produces a heavy-tailed intensity distribution and large scintillation index (a non-central chi-square distribution with two degrees of freedom, also known as the Rice-Nakagami distribution [19]).

In Figures 5 and 6 we illustrate the behavior of the scintillation index in the regime $\ell_s \ll \ell_m$. The figure shows how the scintillation index depends on the magnitudes of the coherence times of the source and of the medium relative to the integration time at the detector. The two figures correspond to two different values for the effective strength of the medium fluctuations

$$\frac{c_2 \sigma_m^2 L^3}{3 \ell_m \ell_s^2}.$$

and we again assume a Gaussian time coherence function f_τ as in (30). Note that in this case the strength parameter does not depend on the central wavelength λ_0 . As above note how strong medium fluctuations serve to reduce the scintillation index in the case with a time-dependent random medium and temporal averaging at the detector, moreover, how again long detector temporal averaging serves to reduce the scintillation index.

5 Example with Experimental Data

We discuss an example with real data taken from the paper [29] by Nelson et al. The experiment in [29] involves an over-the-water laser beam link at the United States Naval Academy. The source is partially coherent (Multi-Gaussian Schell Model) and realized via a SLM. The measurement procedure at the CDD camera corresponds to an averaging interval of $T = 60 \text{sec}$. The experiment is carried out for various values for the source coherence time τ_s realized via varying the SLM cycling rate. The field trials were conducted in July and were performed during the night in calm weather conditions over a maritime link of 323 meters. We refer to the paper [29] for a more detailed description of the experimental setup. Assuming a frozen medium in view of the calm weather we can then model the observed scintillation index as in (25)

$$\mathcal{S} = \frac{2}{T} \int_0^T \left(1 - \frac{\tau}{T}\right) \left[f_\tau^2 + (1 + f_\tau^2) \mathcal{Q}_1(L) \right] d\tau \xrightarrow{\tau_s \ll T} \frac{c_1}{\tau_s^{-1}} + c_2, \quad (32)$$

and we can fit the parameters c_1, c_2 via least squares. The results are shown in Figure 7 and we can see an excellent fit in between model and data.

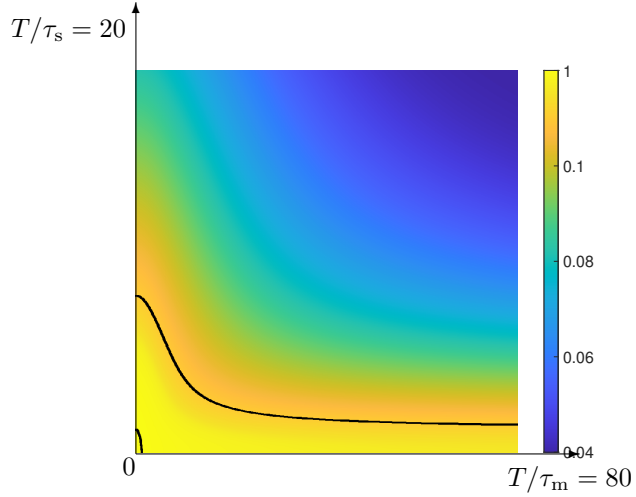


Figure 5: Scintillation index \mathcal{S} as a function of the coherence times of the source and of the random medium, respectively τ_s and τ_m , relative to T , the averaging time at the detector, in the regime $\ell_s \ll \ell_m$. The effective strength parameter for the magnitude of the medium fluctuations is $c_2 \sigma_m^2 L^3 / (3 \ell_m \ell_s^2) = 3$. The two solid black lines correspond to the contour levels $\mathcal{S} = .8$ and $.2$ respectively.

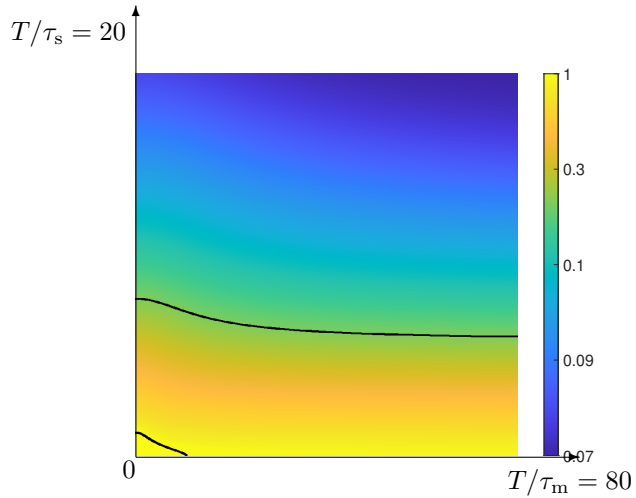


Figure 6: As in Figure 5, however with medium fluctuation strength parameter $c_2 \sigma_m^2 L^3 / (3 \ell_m \ell_s^2) = 1/3$.

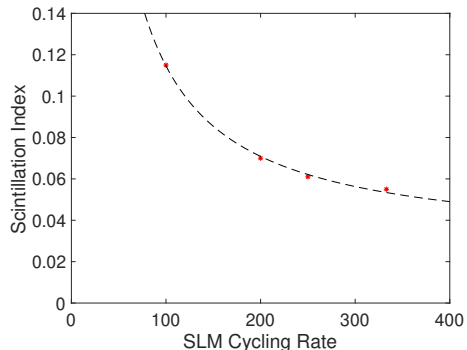


Figure 7: Measurements of scintillation index as function of the SLM cycling rate (red stars). The observations conform well with the theoretical predictions (dashed line) assuming a frozen medium.

6 Conclusions

We have considered the scintillation of wave field that is observed after propagation through a time-dependent random medium. The source is partially coherent in time and space and constitutes a random field in lateral space and time variables. We consider a high-frequency and far-field regime. We give here precise characterizations of the scaling regimes leading to the different canonical forms of scintillation. The central scaling parameters are the temporal and spatial statistical coherence lengths of the source and of the random medium, in addition to the propagation range and the strength of the random medium fluctuations, and the response time of the photodetector. In the high-frequency and far-field regime, three scaling regimes are identified depending on the magnitude of the spatial correlation radius of the source relative to that of the medium. We identify general formulas for the scintillation index in each regime and discuss special cases corresponding to an effective Gaussian situation with scintillation index being equal to one, a non-Gaussian mixture situation with scintillation index reaching beyond one, and situations with small scintillation index corresponding to a desirable high signal-to-noise ratio for the measured intensity. In particular temporal averaging creates situations with a low scintillation index. In the context of for instance communication, however, long averaging times are not in general desirable and our analysis presents quantitative insights about appropriate tradeoffs that can be made for optimal system performance. Such particular system optimization challenges are left for future work. We also remark that we have considered the case when the source has infinite lateral spatial extent and is a stationary stochastic process in lateral space coordinates and time. The case when the source is modulated by a finite source aperture and the associated challenge of identifying the spreading of the wave field and the evolution of speckle statistics can be analyzed via similar theoretical frameworks as those presented here, but is also left for future work.

A Analysis of Fourth-order Moment Equations

The main equation underlying the above results is a simplified equation deriving from (19) and from which the expressions of the special fourth moments $\mu_4(L, \mathbf{0}, \mathbf{0}, \mathbf{0}, \mathbf{0}; \tau)$ follow. We deduce this equation here and analyze it in the specific scintillation regimes in Appendix B.

Consider the general moments in (18) satisfying (19) with initial condition (21). It will be convenient to parameterize the four points $\mathbf{x}_1, \mathbf{x}_2, \mathbf{y}_1, \mathbf{y}_2$ in (18) in the special way:

$$\mathbf{x}_1 = \frac{\mathbf{r}_1 + \mathbf{r}_2 + \mathbf{q}_1 + \mathbf{q}_2}{2}, \quad \mathbf{y}_1 = \frac{\mathbf{r}_1 + \mathbf{r}_2 - \mathbf{q}_1 - \mathbf{q}_2}{2}, \quad (33)$$

$$\mathbf{x}_2 = \frac{\mathbf{r}_1 - \mathbf{r}_2 + \mathbf{q}_1 - \mathbf{q}_2}{2}, \quad \mathbf{y}_2 = \frac{\mathbf{r}_1 - \mathbf{r}_2 - \mathbf{q}_1 + \mathbf{q}_2}{2}. \quad (34)$$

In particular $\mathbf{r}_1/2$ is the barycenter of the four points $\mathbf{x}_1, \mathbf{x}_2, \mathbf{y}_1, \mathbf{y}_2$:

$$\begin{aligned} \mathbf{r}_1 &= \frac{\mathbf{x}_1 + \mathbf{x}_2 + \mathbf{y}_1 + \mathbf{y}_2}{2}, & \mathbf{q}_1 &= \frac{\mathbf{x}_1 + \mathbf{x}_2 - \mathbf{y}_1 - \mathbf{y}_2}{2}, \\ \mathbf{r}_2 &= \frac{\mathbf{x}_1 - \mathbf{x}_2 + \mathbf{y}_1 - \mathbf{y}_2}{2}, & \mathbf{q}_2 &= \frac{\mathbf{x}_1 - \mathbf{x}_2 - \mathbf{y}_1 + \mathbf{y}_2}{2}. \end{aligned}$$

We denote by μ the fourth-order moment in these new variables:

$$\mu(z, \mathbf{q}_1, \mathbf{q}_2, \mathbf{r}_1, \mathbf{r}_2; \tau) = \mu_4(z, \mathbf{x}_1, \mathbf{x}_2, \mathbf{y}_1, \mathbf{y}_2; \tau) \quad (35)$$

with $\mathbf{x}_1, \mathbf{x}_2, \mathbf{y}_1, \mathbf{y}_2$ given by (33-34) in terms of $\mathbf{q}_1, \mathbf{q}_2, \mathbf{r}_1, \mathbf{r}_2$.

In the variables $(\mathbf{q}_1, \mathbf{q}_2, \mathbf{r}_1, \mathbf{r}_2)$ the function μ satisfies the system:

$$\frac{\partial \mu}{\partial z} = \frac{i}{k_o} (\nabla_{\mathbf{r}_1} \cdot \nabla_{\mathbf{q}_1} + \nabla_{\mathbf{r}_2} \cdot \nabla_{\mathbf{q}_2}) \mu + \frac{\sigma_m^2 k_o^2 \ell_m}{4} U(\mathbf{q}_1, \mathbf{q}_2, \mathbf{r}_1, \mathbf{r}_2; \tau) \mu, \quad (36)$$

with the generalized potential

$$\begin{aligned} U(\mathbf{q}_1, \mathbf{q}_2, \mathbf{r}_1, \mathbf{r}_2; \tau) &= C \left(\frac{\mathbf{q}_2 + \mathbf{q}_1}{\ell_m} \right) + C \left(\frac{\mathbf{q}_2 - \mathbf{q}_1}{\ell_m} \right) + g_\tau C \left(\frac{\mathbf{r}_2 + \mathbf{q}_1}{\ell_m} \right) \\ &+ g_\tau C \left(\frac{\mathbf{r}_2 - \mathbf{q}_1}{\ell_m} \right) - g_\tau C \left(\frac{\mathbf{q}_2 + \mathbf{r}_2}{\ell_m} \right) - g_\tau C \left(\frac{\mathbf{q}_2 - \mathbf{r}_2}{\ell_m} \right) - 2. \end{aligned} \quad (37)$$

The Fourier transform (in $\mathbf{q}_1, \mathbf{q}_2, \mathbf{r}_1,$ and \mathbf{r}_2) of the fourth-order moment is defined by:

$$\begin{aligned} \hat{\mu}(z, \boldsymbol{\xi}_1, \boldsymbol{\xi}_2, \boldsymbol{\zeta}_1, \boldsymbol{\zeta}_2; \tau) &= \iint_{\mathbb{R}^2 \times \mathbb{R}^2 \times \mathbb{R}^2 \times \mathbb{R}^2} \mu(z, \mathbf{q}_1, \mathbf{q}_2, \mathbf{r}_1, \mathbf{r}_2; \tau) \\ &\times \exp(-i\mathbf{q}_1 \cdot \boldsymbol{\xi}_1 - i\mathbf{q}_2 \cdot \boldsymbol{\xi}_2 - i\mathbf{r}_1 \cdot \boldsymbol{\zeta}_1 - i\mathbf{r}_2 \cdot \boldsymbol{\zeta}_2) d\mathbf{q}_1 d\mathbf{q}_2 d\mathbf{r}_1 d\mathbf{r}_2. \end{aligned} \quad (38)$$

It satisfies

$$\begin{aligned} \frac{\partial \hat{\mu}}{\partial z} + \frac{i}{k_o} (\boldsymbol{\xi}_1 \cdot \boldsymbol{\zeta}_1 + \boldsymbol{\xi}_2 \cdot \boldsymbol{\zeta}_2) \hat{\mu} &= \frac{\sigma_m^2 k_o^2 \ell_m^3}{4(2\pi)^2} \int_{\mathbb{R}^2} \hat{C}(\mathbf{k} \ell_m) \left[\hat{\mu}(\boldsymbol{\xi}_1 - \mathbf{k}, \boldsymbol{\xi}_2 - \mathbf{k}, \boldsymbol{\zeta}_1, \boldsymbol{\zeta}_2) \right. \\ &+ \hat{\mu}(\boldsymbol{\xi}_1 + \mathbf{k}, \boldsymbol{\xi}_2 - \mathbf{k}, \boldsymbol{\zeta}_1, \boldsymbol{\zeta}_2) - 2\hat{\mu}(\boldsymbol{\xi}_1, \boldsymbol{\xi}_2, \boldsymbol{\zeta}_1, \boldsymbol{\zeta}_2) \\ &+ g_\tau \hat{\mu}(\boldsymbol{\xi}_1 + \mathbf{k}, \boldsymbol{\xi}_2, \boldsymbol{\zeta}_1, \boldsymbol{\zeta}_2 - \mathbf{k}) + g_\tau \hat{\mu}(\boldsymbol{\xi}_1 - \mathbf{k}, \boldsymbol{\xi}_2, \boldsymbol{\zeta}_1, \boldsymbol{\zeta}_2 - \mathbf{k}) \\ &\left. - g_\tau \hat{\mu}(\boldsymbol{\xi}_1, \boldsymbol{\xi}_2 - \mathbf{k}, \boldsymbol{\zeta}_1, \boldsymbol{\zeta}_2 - \mathbf{k}) - g_\tau \hat{\mu}(\boldsymbol{\xi}_1, \boldsymbol{\xi}_2 + \mathbf{k}, \boldsymbol{\zeta}_1, \boldsymbol{\zeta}_2 - \mathbf{k}) \right] d\mathbf{k}, \end{aligned} \quad (39)$$

starting from

$$\begin{aligned} \hat{\mu}(z = 0, \boldsymbol{\xi}_1, \boldsymbol{\xi}_2, \boldsymbol{\zeta}_1, \boldsymbol{\zeta}_2; \tau) &= (2\pi)^8 \phi_{\ell_s^{-1}}(\boldsymbol{\xi}_1) \phi_{\ell_s^{-1}}(\boldsymbol{\xi}_2) \delta(\boldsymbol{\zeta}_1) \delta(\boldsymbol{\zeta}_2) \\ &+ (2\pi)^8 f_\tau^2 \phi_{\ell_s^{-1}}(\boldsymbol{\xi}_1) \phi_{\ell_s^{-1}}(\boldsymbol{\xi}_2) \delta(\boldsymbol{\zeta}_1) \delta(\boldsymbol{\xi}_2). \end{aligned} \quad (40)$$

Here $\hat{C}(\mathbf{q}) = \int_{\mathbb{R}^2} C(\boldsymbol{\chi}) \exp(i\mathbf{q} \cdot \boldsymbol{\chi}) d\boldsymbol{\chi}$ is the Fourier transform of C ,

$$\phi_\kappa(\boldsymbol{\xi}) = \frac{1}{2\pi\kappa^2} \exp\left(-\frac{|\boldsymbol{\xi}|^2}{2\kappa^2}\right), \quad (41)$$

is the 2-dimensional centered isotropic Gaussian density with standard deviation κ , δ is the Dirac delta distribution, and f_τ, g_τ are defined in (17). We now seek to characterize

$$\begin{aligned} \mu_4(L, \mathbf{0}, \mathbf{0}, \mathbf{0}, \mathbf{0}; \tau) &= \mu(L, \mathbf{0}, \mathbf{0}, \mathbf{0}, \mathbf{0}; \tau) \\ &= \frac{1}{(2\pi)^8} \iiint_{\mathbb{R}^2 \times \mathbb{R}^2 \times \mathbb{R}^2 \times \mathbb{R}^2} \hat{\mu}(L, \boldsymbol{\xi}_1, \boldsymbol{\xi}_2, \boldsymbol{\zeta}_1, \boldsymbol{\zeta}_2; \tau) d\boldsymbol{\xi}_1 d\boldsymbol{\xi}_2 d\boldsymbol{\zeta}_1 d\boldsymbol{\zeta}_2. \end{aligned} \quad (42)$$

Thanks to the special initial condition that is proportional to $\delta(\boldsymbol{\zeta}_1)$, the solution $\hat{\mu}$ to (39) is itself proportional to $\delta(\boldsymbol{\zeta}_1)$, and we can therefore reduce the problem (39) to the analysis of

$$\hat{\eta}(z, \boldsymbol{\xi}_2, \boldsymbol{\zeta}_2; \tau) = \frac{1}{(2\pi)^4} \iint_{\mathbb{R}^2 \times \mathbb{R}^2} \hat{\mu}(z, \boldsymbol{\xi}_1, \boldsymbol{\xi}_2, \boldsymbol{\zeta}_1, \boldsymbol{\zeta}_2; \tau) d\boldsymbol{\xi}_1 d\boldsymbol{\zeta}_1. \quad (43)$$

The quantity of interest is then

$$\mu_4(L, \mathbf{0}, \mathbf{0}, \mathbf{0}, \mathbf{0}; \tau) = \frac{1}{(2\pi)^4} \iint_{\mathbb{R}^2 \times \mathbb{R}^2} \hat{\eta}(L, \boldsymbol{\xi}_2, \boldsymbol{\zeta}_2; \tau) d\boldsymbol{\xi}_2 d\boldsymbol{\zeta}_2. \quad (44)$$

The function $\hat{\eta}(z, \boldsymbol{\xi}_2, \boldsymbol{\zeta}_2)$ is solution of the characteristic system

$$\begin{aligned} \frac{\partial \hat{\eta}}{\partial z} + \frac{i}{k_o} \boldsymbol{\xi}_2 \cdot \boldsymbol{\zeta}_2 \hat{\eta} &= \frac{\sigma_m^2 k_o^2 \ell_m^3}{4(2\pi)^2} \int_{\mathbb{R}^2} \hat{C}(\mathbf{k} \ell_m) \left[-2\hat{\eta}(\boldsymbol{\xi}_2, \boldsymbol{\zeta}_2) + 2\hat{\eta}(\boldsymbol{\xi}_2 - \mathbf{k}, \boldsymbol{\zeta}_2) \right. \\ &\left. + 2g_\tau \hat{\eta}(\boldsymbol{\xi}_2, \boldsymbol{\zeta}_2 - \mathbf{k}) - g_\tau \hat{\eta}(\boldsymbol{\xi}_2 - \mathbf{k}, \boldsymbol{\zeta}_2 - \mathbf{k}) - g_\tau \hat{\eta}(\boldsymbol{\xi}_2 + \mathbf{k}, \boldsymbol{\zeta}_2 - \mathbf{k}) \right] d\mathbf{k}, \end{aligned} \quad (45)$$

starting from

$$\hat{\eta}(z=0, \boldsymbol{\xi}_2, \boldsymbol{\zeta}_2; \tau) = (2\pi)^4 \phi_{\ell_s^{-1}}(\boldsymbol{\xi}_2) \delta(\boldsymbol{\zeta}_2) + (2\pi)^4 f_\tau^2 \phi_{\ell_s^{-1}}(\boldsymbol{\zeta}_2) \delta(\boldsymbol{\xi}_2). \quad (46)$$

This simplified system (45-46) underlies the scintillation results presented above. Note that the fourth moment problem has been reduced to a problem defined relative to two, rather than four, copies of the lateral spatial variables. We derive explicit solutions of this system in different scaling regimes in the next Appendix B.

B Derivation of Scintillation Results

As mentioned in Section 2.2, the Itô-Schrödinger equation is valid in the white-noise paraxial regime, when the wavelength is much smaller than the correlation radii of the source and of the medium, which are themselves much smaller than the propagation distance. By the Itô-Schrödinger equation, the fourth-order moment (18) satisfies a closed equation (19). In this section, we derive closed form expressions of the solution of Eq. (19) in three special white-noise paraxial regimes, depending on the ratio of the correlation radii of the source and of the medium.

B.1 Scintillation Regime with a Large Correlation Radius of the Source

We consider the white-noise paraxial regime in which, additionally, the correlation radius of the source is larger than the correlation radius of the medium $\ell_s \gg \ell_m$ and derive the results presented in Section 4.1. More exactly, we here deal with the following scaled regime:

$$\frac{\ell_m}{\ell_s} \sim \varepsilon, \quad \frac{L}{\ell_s} \sim \alpha^{-1}, \quad \frac{\lambda_o}{\ell_s} \sim \alpha \varepsilon, \quad \sigma_m^2 \sim \alpha^3 \varepsilon, \quad (47)$$

and we assume $\alpha \ll \varepsilon \ll 1$ [Note that $L/\ell_{\text{mfp}} \sim 1$ and $\lambda_o L/\ell_m^2 \sim \varepsilon^{-1}$]. This means that the paraxial white-noise limit $\alpha \rightarrow 0$ is taken first (and we get an ε -dependent Itô-Schrödinger equation), and then we want to apply the limit $\varepsilon \rightarrow 0$ in the fourth-moment equation (45). In view of (47) it is natural to introduce the rescaled function

$$\tilde{\eta}^\varepsilon(z, \boldsymbol{\xi}_2, \boldsymbol{\zeta}_2; \tau) = \hat{\eta}\left(\frac{z}{\varepsilon}, \boldsymbol{\xi}_2, \boldsymbol{\zeta}_2; \tau\right) \exp\left(i \frac{z}{\varepsilon k_o} \boldsymbol{\xi}_2 \cdot \boldsymbol{\zeta}_2\right). \quad (48)$$

In the regime (47) the rescaled function $\tilde{\eta}^\varepsilon$ satisfies the equation with fast phases

$$\frac{\partial \tilde{\eta}^\varepsilon}{\partial z} = \mathcal{L}_z^\varepsilon \tilde{\eta}^\varepsilon, \quad (49)$$

where

$$\begin{aligned} \mathcal{L}_z^\varepsilon \tilde{\eta}(\boldsymbol{\xi}_2, \boldsymbol{\zeta}_2) &= \frac{\sigma_m^2 k_o^2 \ell_m^3}{4(2\pi)^2} \int_{\mathbb{R}^2} \hat{C}(\mathbf{k} \ell_m) \left[-2\tilde{\eta}(\boldsymbol{\xi}_2, \boldsymbol{\zeta}_2) + 2\tilde{\eta}(\boldsymbol{\xi}_2 - \mathbf{k}, \boldsymbol{\zeta}_2) e^{i \frac{z}{\varepsilon k_o} \mathbf{k} \cdot \boldsymbol{\zeta}_2} \right. \\ &+ 2g_\tau \tilde{\eta}(\boldsymbol{\xi}_2, \boldsymbol{\zeta}_2 - \mathbf{k}) e^{i \frac{z}{\varepsilon k_o} \mathbf{k} \cdot \boldsymbol{\xi}_2} - g_\tau \tilde{\eta}(\boldsymbol{\xi}_2 - \mathbf{k}, \boldsymbol{\zeta}_2 - \mathbf{k}) e^{i \frac{z}{\varepsilon k_o} (\mathbf{k} \cdot (\boldsymbol{\zeta}_2 + \boldsymbol{\xi}_2) - |\mathbf{k}|^2)} \\ &\left. - g_\tau \tilde{\eta}(\boldsymbol{\xi}_2 - \mathbf{k}, \boldsymbol{\zeta}_2 + \mathbf{k}) e^{i \frac{z}{\varepsilon k_o} (\mathbf{k} \cdot (\boldsymbol{\zeta}_2 - \boldsymbol{\xi}_2) + |\mathbf{k}|^2)} \right] d\mathbf{k}, \end{aligned} \quad (50)$$

and the initial condition is

$$\tilde{\eta}^\varepsilon(z=0, \boldsymbol{\xi}_2, \boldsymbol{\zeta}_2; \tau) = (2\pi)^4 \phi_{\varepsilon/\ell_s}(\boldsymbol{\xi}_2) \delta(\boldsymbol{\zeta}_2) + (2\pi)^4 f_\tau^2 \phi_{\varepsilon/\ell_s}(\boldsymbol{\zeta}_2) \delta(\boldsymbol{\xi}_2). \quad (51)$$

Note that ϕ_κ belongs to L^1 and has a L^1 -norm equal to one. The asymptotic behavior as $\varepsilon \rightarrow 0$ of the moments is therefore determined by the solutions of partial differential equations with rapid phase terms. We can now proceed as in [20] and we obtain the following proposition.

Proposition B.1 *In the regime (47), the function $\tilde{\eta}^\varepsilon(z, \boldsymbol{\xi}_2, \boldsymbol{\zeta}_2; \tau)$ has the form*

$$\begin{aligned} \tilde{\eta}^\varepsilon(z, \boldsymbol{\xi}_2, \boldsymbol{\zeta}_2; \tau) &= K(z) \phi_{\varepsilon/\ell_s}(\boldsymbol{\xi}_2) \delta(\boldsymbol{\zeta}_2) + K(z) A_1(z, \boldsymbol{\xi}_2, \mathbf{0}) \delta(\boldsymbol{\zeta}_2) \\ &+ K(z) A_{g_\tau}(z, \boldsymbol{\zeta}_2, \frac{\boldsymbol{\xi}_2}{\varepsilon}) \phi_{\varepsilon/\ell_s}(\boldsymbol{\xi}_2) + f_\tau^2 K(z) \delta(\boldsymbol{\xi}_2) \phi_{\varepsilon/\ell_s}(\boldsymbol{\zeta}_2) \\ &+ f_\tau^2 K(z) A_{g_\tau}(z, \boldsymbol{\zeta}_2, \mathbf{0}) \delta(\boldsymbol{\xi}_2) + f_\tau^2 K(z) A_1(z, \boldsymbol{\xi}_2, \frac{\boldsymbol{\zeta}_2}{\varepsilon}) \phi_{\varepsilon/\ell_s}(\boldsymbol{\zeta}_2) \\ &+ R^\varepsilon(z, \boldsymbol{\xi}_2, \boldsymbol{\zeta}_2; \tau), \end{aligned} \quad (52)$$

where the functions K and A_g are defined by

$$K(z) = (2\pi)^4 \exp\left(-\frac{\sigma_m^2 k_o^2 \ell_m z}{2}\right), \quad (53)$$

$$\begin{aligned} A_g(z, \boldsymbol{\xi}, \boldsymbol{\zeta}) &= \frac{1}{(2\pi)^2} \int_{\mathbb{R}^2} \left[\exp\left(\frac{\sigma_m^2 k_o^2 \ell_m g}{2} \int_0^z C\left(\frac{\mathbf{x}}{\ell_m} + \frac{\boldsymbol{\zeta} z'}{k_o \ell_m}\right) dz'\right) - 1 \right] \\ &\times \exp(-i \boldsymbol{\xi} \cdot \mathbf{x}) d\mathbf{x}, \end{aligned} \quad (54)$$

and the function R^ε satisfies $\sup_{z \in [0, L]} \|R^\varepsilon(z, \cdot, \cdot; \tau)\|_{L^1(\mathbb{R}^2 \times \mathbb{R}^2)} \xrightarrow{\varepsilon \rightarrow 0} 0$.

We remark that

$$\frac{K^{1/4}(z)}{2\pi} = \exp\left(-\frac{\sigma_m^2 k_o^2 \ell_m z}{8}\right) \quad (55)$$

represents damping of the mean wave field due to scattering and transfer of coherent energy to incoherent wave energy in the case with frozen medium and deterministic sources. We remark moreover that the factor A_g depends on the two point statistics of the random medium at lateral offsets and captures effects of lateral scattering of wave field energy. As a result, the quantity of interest in (44) is then

$$\mu_4^\varepsilon(L, \mathbf{0}, \mathbf{0}, \mathbf{0}; \tau) = 1 + f_\tau^2 \exp\left(-\frac{\sigma_m^2 (1 - g_\tau) k_o^2 \ell_m L}{2}\right) + \mathcal{Q}_{g_\tau}(L) + f_\tau^2 \mathcal{Q}_1(L) \quad (56)$$

with

$$\begin{aligned} \mathcal{Q}_g(L) &= \exp\left(-\frac{\sigma_m^2 k_o^2 \ell_m L}{2}\right) \int_{\mathbb{R}^2} \phi_{\ell_s^{-1}}(\zeta) \\ &\times \left[\exp\left(\frac{\sigma_m^2 k_o^2 \ell_m g}{2} \int_0^L C\left(\frac{\zeta z}{k_o \ell_m}\right) dz\right) - 1 \right] d\zeta. \end{aligned} \quad (57)$$

Therefore the relative covariance of the intensities at time zero and time τ is

$$\begin{aligned} \frac{\mu_4^\varepsilon(L, \mathbf{0}, \mathbf{0}, \mathbf{0}; \tau) - \mu_2^\varepsilon(L, \mathbf{0}, \mathbf{0}; 0)^2}{\mu_2^\varepsilon(L, \mathbf{0}, \mathbf{0}; 0)^2} &= f_\tau^2 \exp\left(-\frac{\sigma_m^2 (1 - g_\tau) k_o^2 \ell_m L}{2}\right) \\ &+ \mathcal{Q}_{g_\tau}(L) + f_\tau^2 \mathcal{Q}_1(L). \end{aligned}$$

This gives the result (23) for the scintillation index in the regime $\ell_s \gg \ell_m$.

B.2 Scintillation Regime with an Intermediate Correlation Radius of the Source

We consider the white-noise paraxial regime in which, additionally, the correlation radius of the source is of the same order as the correlation radius of the medium $\ell_s \sim \ell_m$. This is the regime when the source lateral spatial fluctuations takes place on the same scale of variation as that of the random microstructure fluctuations, rather than being large relative to this scale as in the previous Section B.1. More exactly, we here deal with the following scaled regime:

$$\frac{\ell_m}{\ell_s} \sim 1, \quad \frac{L}{\ell_s} \sim \alpha^{-1} \varepsilon^{-1}, \quad \frac{\lambda_o}{\ell_s} \sim \alpha, \quad \sigma_m^2 \sim \alpha^3 \varepsilon, \quad (58)$$

and we assume $\alpha \ll \varepsilon \ll 1$ [Note that $L/\ell_{\text{mfp}} \sim 1$ and $\lambda_o L/\ell_m^2 \sim \varepsilon^{-1}$]. This means that the paraxial white-noise limit $\alpha \rightarrow 0$ is taken first, and then we want to apply the limit $\varepsilon \rightarrow 0$ in the fourth-moment equation (45). As above we introduce the rescaled function

$$\tilde{\eta}^\varepsilon(z, \boldsymbol{\xi}_2, \boldsymbol{\zeta}_2; \tau) = \hat{\eta}\left(\frac{z}{\varepsilon}, \boldsymbol{\xi}_2, \boldsymbol{\zeta}_2; \tau\right) \exp\left(i \frac{z}{k_o \varepsilon} \boldsymbol{\xi}_2 \cdot \boldsymbol{\zeta}_2\right). \quad (59)$$

In the regime (58) the rescaled function $\tilde{\eta}^\varepsilon$ satisfies again the equation with fast phases (49-50), here with initial condition given by (46). The asymptotic behavior as $\varepsilon \rightarrow 0$ of the moments is therefore determined by the solutions of partial differential equations with rapid phase terms. We can again proceed similarly as in [20] and we obtain the following proposition.

Proposition B.2 *In the scintillation regime (58), the function $\tilde{\eta}^\varepsilon(z, \boldsymbol{\xi}_2, \boldsymbol{\zeta}_2; \tau)$ has the form*

$$\tilde{\eta}^\varepsilon(z, \boldsymbol{\xi}_2, \boldsymbol{\zeta}_2; \tau) = (2\pi)^4 B_1(z, \boldsymbol{\xi}_2) \delta(\boldsymbol{\zeta}_2) + (2\pi)^4 f_\tau^2 B_{g_\tau}(z, \boldsymbol{\zeta}_2) \delta(\boldsymbol{\xi}_2) + R^\varepsilon(z, \boldsymbol{\xi}_2, \boldsymbol{\zeta}_2; \tau), \quad (60)$$

with

$$B_g(z, \boldsymbol{\xi}) = \frac{1}{(2\pi)^2} \int_{\mathbb{R}^2} \exp\left(-i\boldsymbol{\xi} \cdot \mathbf{x} - \frac{|\mathbf{x}|^2}{2\ell_s^2} - \frac{\sigma_m^2 k_o^2 \ell_m z}{2} \left[1 - gC\left(\frac{\mathbf{x}}{\ell_m}\right)\right]\right) d\mathbf{x}, \quad (61)$$

and the function R^ε satisfies $\sup_{z \in [0, L]} \|R^\varepsilon(z, \cdot, \cdot; \tau)\|_{L^1(\mathbb{R}^2 \times \mathbb{R}^2)} \xrightarrow{\varepsilon \rightarrow 0} 0$.

As a result, the quantity of interest (44) is

$$\mu_4^\varepsilon(L, \mathbf{0}, \mathbf{0}, \mathbf{0}, \mathbf{0}; \tau) = 1 + f_\tau^2 \exp\left(-\frac{\sigma_m^2(1-g_\tau)k_o^2 \ell_m L}{2}\right) \quad (62)$$

and

$$\frac{\mu_4^\varepsilon(L, \mathbf{0}, \mathbf{0}, \mathbf{0}, \mathbf{0}; \tau) - \mu_2^\varepsilon(L, \mathbf{0}, \mathbf{0}; 0)^2}{\mu_2^\varepsilon(L, \mathbf{0}, \mathbf{0}; 0)^2} = f_\tau^2 \exp\left(-\frac{\sigma_m^2(1-g_\tau)k_o^2 \ell_m L}{2}\right). \quad (63)$$

This then gives the result (29) for the scintillation index.

B.3 Scintillation Regime with a Small Correlation Radius of the Source

We finally consider the white-noise paraxial regime in which, additionally, the correlation radius of the source is smaller than the correlation radius of the medium $\ell_s \ll \ell_m$ and derive the result (31) for the scintillation index in this regime. More exactly, we here deal with the following scaled regime:

$$\frac{\ell_m}{\ell_s} \sim \varepsilon^{-1}, \quad \frac{L}{\ell_s} \sim \alpha^{-1}, \quad \frac{\lambda_o}{\ell_s} \sim \alpha, \quad \sigma_m^2 \sim \alpha^3 \varepsilon^{-1}, \quad (64)$$

and we assume $\alpha \ll \varepsilon \ll 1$ [Note that $L/\ell_{\text{mfp}} \sim \varepsilon^{-2}$ and $\lambda_o L/\ell_s^2 \sim 1$]. This means that the paraxial white-noise limit $\alpha \rightarrow 0$ is taken first, and then we want to apply the limit $\varepsilon \rightarrow 0$ in the fourth-moment equation (45). We also assume that C is smooth and isotropic, so that we have (28), and also $\frac{1}{(2\pi)^2} \int_{\mathbb{R}^2} \hat{C}(\mathbf{q}) \mathbf{q} \otimes \mathbf{q} d\mathbf{q} = 2c_2 \mathbf{I}$. We denote by $\hat{\eta}^\varepsilon$ the function (43) in the regime (64). Then we find that in the regime of small ε the function $\hat{\eta}^\varepsilon(z, \boldsymbol{\xi}_2, \boldsymbol{\zeta}_2; \tau)$ is solution to the system

$$\frac{\partial \hat{\eta}^\varepsilon}{\partial z} + \frac{i}{k_o} \boldsymbol{\xi}_2 \cdot \boldsymbol{\zeta}_2 \hat{\eta}^\varepsilon = \frac{\sigma_m^2 k_o^2 c_2 (1-g_\tau)}{2\ell_m} \Delta_{\boldsymbol{\xi}_2} \hat{\eta}^\varepsilon, \quad (65)$$

with initial condition given by (46). We can easily solve (65) via a Fourier transform and find

Proposition B.3 *In the scintillation regime (64), the function $\hat{\eta}^\varepsilon(z, \boldsymbol{\xi}_2, \boldsymbol{\zeta}_2; \tau)$ has the form*

$$\hat{\eta}^\varepsilon(z, \boldsymbol{\xi}_2, \boldsymbol{\zeta}_2; \tau) = (2\pi)^4 G_1(z, \boldsymbol{\xi}_2; \tau) \delta(\boldsymbol{\zeta}_2) + (2\pi)^4 f_\tau^2 G_2(z, \boldsymbol{\xi}_2, \boldsymbol{\zeta}_2; \tau) \phi_{1/\ell_s}(\boldsymbol{\zeta}_2), \quad (66)$$

with

$$G_1(z, \boldsymbol{\xi}_2; \tau) = \frac{\ell_s^2}{2\pi} \frac{1}{1 + \frac{\sigma_m^2(1-g_\tau)c_2k_o^2\ell_s^2L}{\ell_m}} \exp\left(-\frac{\ell_s^2|\boldsymbol{\xi}_2|^2}{2\left(1 + \frac{\sigma_m^2(1-g_\tau)c_2k_o^2\ell_s^2L}{\ell_m}\right)}\right), \quad (67)$$

$$\begin{aligned} G_2(z, \boldsymbol{\xi}_2, \boldsymbol{\zeta}_2; \tau) &= \frac{1}{(2\pi)^2} \int_{\mathbb{R}^2} \exp\left(-\frac{c_2(1-g_\tau)\sigma_m^2k_o^2}{2\ell_m} \int_0^L \left|\mathbf{x} - \frac{\boldsymbol{\zeta}_2 z}{k_o}\right|^2 dz - i\boldsymbol{\xi}_2 \cdot \mathbf{x}\right) d\mathbf{x} \\ &= \frac{\ell_m}{2\pi c_2(1-g_\tau)\sigma_m^2k_o^2L} \exp\left(-\frac{iL}{2k_o}\boldsymbol{\xi}_2 \cdot \boldsymbol{\zeta}_2\right) \\ &\quad \times \exp\left(-\frac{c_2(1-g_\tau)\sigma_m^2L^3}{24\ell_m}|\boldsymbol{\zeta}_2|^2 - \frac{\ell_m}{2c_2(1-g_\tau)\sigma_m^2k_o^2L}|\boldsymbol{\xi}_2|^2\right). \end{aligned} \quad (68)$$

As a result

$$\mu_4^\varepsilon(L, \mathbf{0}, \mathbf{0}, \mathbf{0}, \mathbf{0}; \tau) = 1 + \frac{f_\tau^2}{1 + \frac{c_2(1-g_\tau)\sigma_m^2L^3}{3\ell_m\ell_s^2}} \quad (69)$$

and

$$\frac{\mu_4^\varepsilon(L, \mathbf{0}, \mathbf{0}, \mathbf{0}, \mathbf{0}; \tau) - \mu_2^\varepsilon(L, \mathbf{0}, \mathbf{0}; 0)^2}{\mu_2^\varepsilon(L, \mathbf{0}, \mathbf{0}; 0)^2} = \frac{f_\tau^2}{1 + \frac{c_2(1-g_\tau)\sigma_m^2L^3}{3\ell_m\ell_s^2}}. \quad (70)$$

This then gives (31) for the scintillation index when $\ell_s \ll \ell_m$.

Funding

JG was supported by the Agence Nationale pour la Recherche under Grant No. ANR-19-CE46-0007 (project ICCI), and Air Force Office of Scientific Research under grant FA9550-18-1-0217.

KS was supported by the Air Force Office of Scientific Research under grant FA9550-18-1-0217, and the National Science Foundation under grant DMS-2010046.

Acknowledgments

We thank C. Nelson, S. Avramov-Zamurovic, O. Korotkova, S. Guth and R. Malek-Madani for allowing us to use their data from [29] to generate Figure 7.

References

- [1] L. C. Andrews and R. L. Philipps, *Laser Beam Propagation Through Random Media*, SPIE Press, Bellingham, 2005. 2

- [2] S. Avramov-Zamurovic, C. Nelson, S. Guth and O. Korotkova, Flatness parameter influence on scintillation reduction for multi-Gaussian Schell-model beams propagating in turbulent air, *Applied Optics* **55:13** 3442–3446 (2016). [3](#), [5](#)
- [3] G. Baker, Gaussian beam weak scintillation: low-order turbulence effects and applicability of the Rytov method, *J. Opt. Soc. Am. A* **23:2** 395–417 (2006). [3](#)
- [4] G. Bal, T. Komorowski, and L. Ryzhik, Asymptotics of the solutions of the random Schrödinger equation, *Arch. Rational Mech. Anal.* **200** 613–664 (2011). [4](#)
- [5] G. Bal and O. Pinaud, Dynamics of wave scintillation in random media, *Comm. Partial Differential Equations* **35** 1176–1235 (2010). [3](#)
- [6] V. A. Banach, V. M. Buldakov, and V. L. Mironov, Intensity fluctuations of the partially coherent light-beam in a turbulent atmosphere, *Opt. Spectrosc.* **54:6** 1054–1059 (1983). [3](#)
- [7] V. A. Banakh and V. M. Buldakov, Effect of the initial degree of light-beam spatial coherence on intensity fluctuations in turbulent atmospheres, *Opt. Spectrosc.* **55:4** 707–712 (1983). [3](#)
- [8] M. Charnotskii, Extended Huygens-Fresnel principle and optical waves propagation in turbulence: discussion, *J. Opt. Soc. Am. A* **32:7** 1357–1365 (2015). [3](#)
- [9] M. Charnotskii, Beam scintillations for ground-to-space propagation. Part I: Path integrals and analytic techniques, *J. Opt. Soc. Am. A* **27:10** 2169–2179 (2010). [3](#)
- [10] J. C. Dainty, *Laser Speckle and Related Phenomena*, Springer-Verlag, Berlin, Topics in Applied Physics, Volume 9, 1975. [2](#)
- [11] D. Dawson and G. Papanicolaou, A random wave process, *Appl. Math. Optim.* **12** 97–114 (1984). [9](#)
- [12] R. L. Fante, The effect of source temporal coherence on light scintillations in weak turbulence, *J. Opt. Soc. Am.* **69** 71–73 (1979). [3](#)
- [13] R. L. Fante, Intensity fluctuations of an optical wave in a turbulent medium effect of source coherence, *Optica Acta* **28:9** 1203–1207 (1981). [3](#)
- [14] J.-P. Fouque, J. Garnier, G. Papanicolaou, and K. Sølna, *Wave Propagation and Time Reversal in Randomly Layered Media*, Springer, New York, 2007. [4](#)
- [15] J.-P. Fouque, G. Papanicolaou, and Y. Samuelides, Forward and Markov approximation: the strong-intensity-fluctuations regime revisited, *Waves in Random Media* **8** 303–314 (1998). [9](#)

- [16] K. Furutsu and Y. Furuhashi, Spot dancing and relative saturation phenomena of irradiance scintillation of optical beams in a random medium, *Optica* **20** 707–719 (1973). [15](#)
- [17] J. Garnier, C. Gouédard, and L. Videau, Propagation of a partially coherent beam under the interaction of small and large scales, *Optics Communications* **176** 281–297 (2000).
- [18] J. Garnier and K. Sølna, Scaling limits for wave pulse transmission and reflection operators, *Wave Motion* **46** 122–143 (2009).
- [19] J. Garnier and K. Sølna, Scintillation in the white-noise paraxial regime, *Comm. Part. Differ. Equat.* **39** 626–650 (2014). [3](#), [6](#), [7](#), [8](#), [15](#), [16](#)
- [20] J. Garnier and K. Sølna, Fourth-moment analysis for beam propagation in the white-noise paraxial regime, *Arch. Rational Mech. Anal.* **220** 37–81 (2016). [3](#), [9](#), [10](#), [22](#), [23](#)
- [21] J. Garnier and K. Sølna, Coupled paraxial wave equations in random media in the white-noise regime, *Ann. Appl. Probab.* **19** 318–346 (2009). [6](#), [7](#)
- [22] J. Garnier and K. Sølna, Scaling limits for wave pulse transmission and reflection operators, *Wave Motion* **46** 122–143 (2009). [7](#)
- [23] J. Garnier and K. Sølna, Imaging through a scattering medium by speckle intensity correlations, *Inverse Problems* **34** 094003 (2018). [8](#)
- [24] J. Garnier and K. Sølna, Focusing waves through a randomly scattering medium in the white-noise paraxial regime, *SIAM J. Appl. Math.* **77** 500–519 (2017). [5](#)
- [25] J. Garnier and K. Sølna, Beaming Through Turbulence, *OSA Technical Digest* paper PTh2D.4 (2019). [6](#)
- [26] G. Gbur, Partially coherent beam propagation in atmospheric turbulence, *J. Opt. Soc. Am. A* **31:9** 2038–2045 (2014). [3](#)
- [27] H. Gerçekcioglu and Y. Baykal, Minimization of the scintillation index of sinusoidal Gaussian beams in weak turbulence for aerial vehicle-satellite laser communications, *J. Opt. Soc. Am. A* **38:6** 862–868 (2021). [3](#)
- [28] Y. Gu and T. Komorowski, Gaussian fluctuations from random Schrödinger equation, *Comm. Part. Differ. Equat.* **46:2** 201–232 (2021). [4](#)
- [29] C. Nelson, S. Avramov-Zamurovic, O. Korotkova, S. Guth, and R. Malek-Madani, Scintillation reduction in pseudo Multi-Gaussian Schell Model Beams in the maritime environment, *Optics Communications* **364** 145–149 (2016). [3](#), [5](#), [8](#), [16](#), [25](#)

- [30] X. Shan, C. Menyuk, J. Chen, and Y. Ai, Scintillation index analysis of an optical wave propagating through the moderate-to-strong turbulence in satellite communication links, *Optics Communications* **445** 255–261 (2019). [3](#)
- [31] S. E. J. Shaw, Scintillation averaging and fade statistics, *J. Opt. Soc. Am. A* **37:5** 833–840 (2020). [3](#)
- [32] V. I. Tatarskii, A. Ishimaru, and V. U. Zavorotny, eds., *Wave Propagation in Random Media (Scintillation)*, SPIE Press, Bellingham, 1993. [2](#)
- [33] G. C. Valley and D. L. Knepp, Application of joint Gaussian statistics to interplanetary scintillation, *J. Geophys. Res.* **81** 4723–4730 (1976). [4](#)
- [34] D. Voelz and K. Fitzhenry, Pseudo-partially coherent beam for free-space laser communication, *Proc. of SPIE* **5550** 218–224 (2004). [5](#)
- [35] X. Xiao and D. Voltz, Wave optics simulation approach for partially spatially coherent beams, *Opt. Exp.* **14:16** 6986–6992 (2006). [3](#)
- [36] G. Xu, Z. Song, and Q. Zhang, Outage probability and channel capacity of an optical spherical wave propagating through anisotropic weak-to-strong oceanic turbulence with Málaga distribution, *J. Opt. Soc. Am. A* **37:10** 1622–1629 (2020). [3](#)
- [37] I. G. Yakushkin, Moments of field propagating in randomly inhomogeneous medium in the limit of saturated fluctuations, *Radiophys. Quantum Electron.* **21** 835–840 (1978). [4](#)